CrossMark

ORIGINAL PAPER

The effects of two biocompatible plasticizers on the performance of dry bacterial cellulose membrane: a comparative study

Yi Sun · Chunmei Meng · Yudong Zheng (ID) **· Yajie Xie · Wei He ·
Yansen Wang · Kun Qiao · Lina Yue**

Abstract Bacterial cellulose (BC) has unique properties and is widely applied as wound dressings. Dry BC membranes have better stability and longer storage time, but are poor in gas permeability and water absorption. To solve the problems with dry BC, we prepared two different plasticized dry BC membranes using two biocompatible plasticizers with different molecular weight and hydroxyl content, namely glycerol (G) and polyethylene glycol (PEG). The different effects of the two plasticizers on the structure and performance of dry BC were systematically compared and analyzed. The plasticized dry BC membranes were characterized with Fourier transform infrared spectroscopy, scanning electron microscopy, thermo-gravimetry, etc. The elongation at break for BC/2%G and BC/2%PEG were 8.1 and 12.5 times that of dry BC, respectively. BC/2%G had a water absorption of 4560%, and a water retention rate of 2468%, and those for BC/2%PEG were 4690% and 1972%, respectively. The highly porous structure of the plasticized dry BC membranes effectively enhanced the water vapor transmission rate of the membranes. The different effects of the two plasticizers can be ascribed to the differences in molecule size, hydroxyl content, hydrogen bond interaction, etc. The plasticized dry BC membranes showed excellent resistance to bacteria, which were 99.8% for BC/G and 99.9% for BC/PEG. The performance of the two plasticized dry BC membranes can be tuned to adapt to different applications.

Yi Sun and Chunmei Meng have contributed equally to this work and should be considered as co-first authors.

Y. Sun · C. Meng · Y. Zheng (✉) ·
Y. Xie · W. He · Y. Wang · K. Qiao · L. Yue
School of Materials Science and Engineering, University of Science and Technology Beijing, Beijing 100083, People's Republic of China
e-mail: zhengyudong@mater.ustb.edu.cn

Graphical Abstract
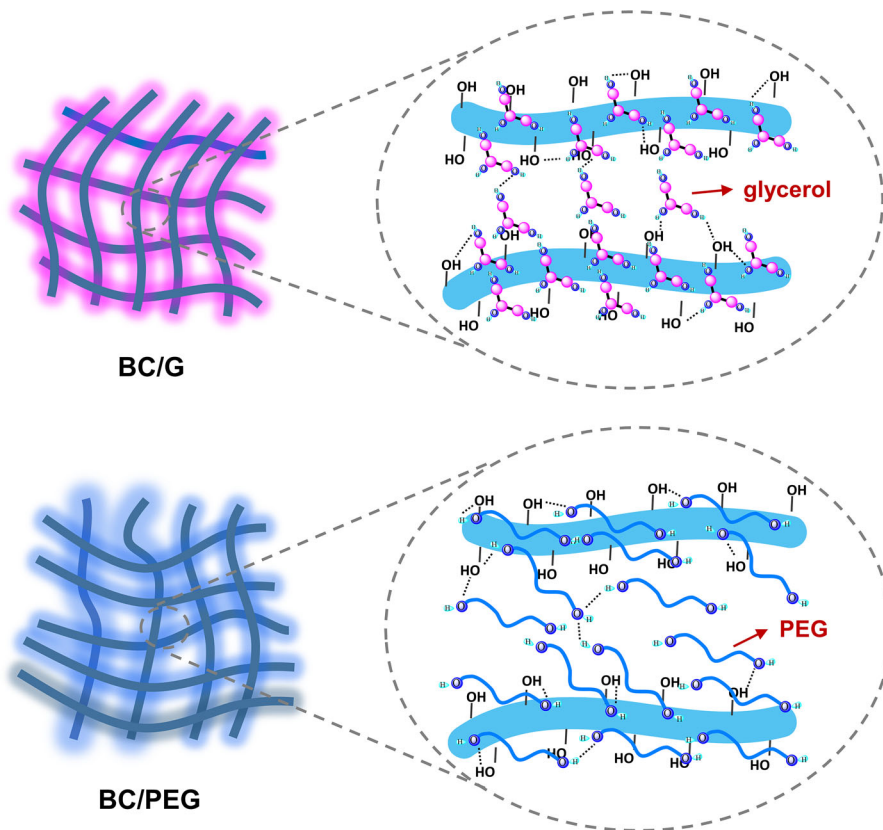
BC/G

BC/PEG

Abbreviations

BC	Bacterial cellulose (without special instruction, BC in this paper is in dry state)
G	Glycerol
PEG	Polyethylene glycol
E%	The elongation at break
WVT	Water vapor transmission rate
WA	Water absorption capacity
WR	Water retention rate
RB	Rate of resistance to bacteria

Introduction

Bacterial cellulose (BC) is an extracellular polysaccharide generated by microorganisms such as *Gluconacetobacter xylinum*. It features a unique ultra-fine three-dimensional nano network, a high specific surface area, high hydroscopicity and water retention capacity, good mechanical properties and good biocompatibility. In addition, the large amounts of hydroxyl groups present in BC facilitate the diverse expansion of its functions. Due to these merits, BC has been widely used in a variety of fields, such as tissue engineering (Andrade et al. 2010; Luo et al. 2014; Stumpf et al. 2016; Wang et al. 2018), wound dressings (Qiao et al. 2017; Sulaeva et al. 2015; Ye et al. 2018), food industry (Díaz-Calderón et al. 2018), waste water treatment (Li et al. 2018; Urbina et al. 2018; Yang et al. 2018), flexible electrodes(Sun et al. 2017; Wan et al. 2015), and supercapacitors (Bu et al. 2018; Zhang et al. 2018). Among these applications, BC has been extensively studied as wound dressings. An ideal wound dressing should maintain a moist environment at the wound surface, allow gaseous exchange, act as a barrier against microorganisms and be flexible enough to adapt to the wound. It should also be non-toxic, non-allergenic, and non-adherent. In

addition, it should be able to lock exudates from the wound and can be easily removed (Jayakumar et al. 2011; Khamrai et al. 2017; Lamboni et al. 2016; Liakos et al. 2015; Sarhan et al. 2016; Sulaeva et al. 2015).

BC can provide a moist healing environment and serve as an effective physical barrier against external infection (Cui et al. 2014). The highly porous structure of BC allows for the potential transfer of antibiotics or other medication into the wound (Lin et al. 2015). Furthermore, BC gel does not adhere to the wounds, which prevents secondary damage. These features make BC a good wound dressing material. Wu and co-workers prepared a slow-released antimicrobial wound dressing by growing silver nanoparticles onto the nanofibers of BC (Wu et al. 2014b). The wound dressing exhibited significant antibacterial properties with more than 99% reductions in *Escherichia coli*, *Staphylococcus aureus* and *Pseudomonas aeruginosa*. Moreover, it supported the attachment and growth of epidermal cells without sign of cytotoxicity (Wu et al. 2014a). Other examples of BC-based wound dressings include BC-vaccarin membranes (Qiu et al. 2016) and tetracycline hydrochloride-loaded BC composite membranes (Shao et al. 2016).

However, in its hydrogel state, the properties of BC-based wound dressings are not stable, which limits their storage time. Additionally, they are poor in gas permeability and wound fluid absorption. To overcome these problems, work has been done to develop wound dressings based on dry BC membranes. Dry BC-based wound dressings have better stability, gas permeability and mechanical strength. However, the water reabsorbing capacity and water retention capacity of dry BC membranes are severely compromised, which is disadvantageous for their use as wound dressings. Furthermore, BC membranes are also brittle. To cope with these problems, plasticizers were subsequently introduced.

Plasticizers help to decrease inherent brittleness of films by reducing intermolecular forces, increasing the mobility of polymer chains, decreasing the glass transition temperature of these materials and improving their flexibility (Azadimanesh and Mohammadi 2015). Common plasticizers include monosaccharides, oligosaccharides, polyols, lipids, etc. (Cobos et al. 2017; Sanyang et al. 2015). Among these, glycerol and poly(ethylene glycol) (PEG) have shown significant potential. Glycerol is a well-known

biocompatible polyol and has been used as a plasticizer. Silva et al. prepared a transdermal delivery systems based on BC by using glycerol as a plasticizer. The membrane showed good flexibility and a considerably higher swelling behavior compared with pure BC (Silva et al. 2014). Almeida and co-workers evaluated the skin irritation potential of glycerol-plasticized BC in human subjects. They found no significant differences for transepidermal water loss measurements in comparison with negative control; similar results were found for erythema (Almeida et al. 2013). PEG is a biocompatible synthetic polymer with wide application in biotechnology and medicine. It has also been used as a plasticizer. Cai et al. prepared a BC/PEG composite by immersing a wet BC pellicle in a PEG aqueous solution followed by a freeze-drying process. 3T3 fibroblast cells incubation experiments showed that BC/PEG had much better biocompatibility than the pure BC. However, the BC/PEG composite showed typical brittle properties, which is probably due to the freeze-drying process (Cai and Kim 2010). In a short communication, Numata et al. reported the shape-memory property of BC compounded with PEG200 and PEG1000 mixture (Numata et al. 2009). In another work, Supamas Napavichayanun et al. prepared a BC composite incorporated with silk sericin, polyhexamethylene biguanide and glycerin, and evaluated its potential as wound dressing (Napavichayanun et al. 2018). However, although there have been studies using PEG or glycerol to plasticize BC, the structure of the plasticized BC and its performance as wound dressing have not been systematically studied. Especially, the effect of plasticizers with different molecular weight or hydroxyl content on the performance of dry BC membrane has not been studied or compared.

The purpose of this paper is to prepare plasticized dry BC membranes with plasticizers of different molecular weight or hydroxyl content, namely glycerol and PEG, and systematically compare the different effects of the two plasticizers on the structure and performance of dry BC membranes. The plasticized dry BC membranes were prepared by the soaking method and then characterized with FT-IR, SEM, TG, etc. The mechanical strength, water absorption, water retention properties, water vapor transmission rate and resistance against bacteria of the two membranes were studied and compared. The mechanisms of how

different plasticizers affect the performance of the plasticized dry BC membranes were also discussed.

Experimental

Materials

Bacterial cellulose membranes produced by *Gluconacetobacter xylinus* were obtained from Hainan Yide Food Co., Ltd. The membrane was 3 mm thick in its moist condition, with a moisture content of about 13,000%. Sodium hydroxide (NaOH) was purchased from Sinopharm Chemical Reagent Beijing Co., Ltd. Poly (ethylene glycol) (PEG 200) was purchased from COOLABER SCIENCE & TECHNOLOGY. Glycerol was obtained from Sinopharm Chemical Reagent Co., Ltd. The bacterial strain of *Staphylococcus aureus* (ATCC6538) was obtained from Shanghai shengwu.com. Mannitol Salt Agar was purchased from Qingdao Hope Bio-Technology Co., Ltd. All reagents were of analysis pure and used as received.

Preparation of the plasticized dry BC membranes

The BC membranes were washed with distilled water. The membranes were then immersed in a 0.1 M NaOH solution and water-bath heated at 90 °C for 1 h to remove the biomass from the membranes. After that, the members were washed with distilled water to pH = 7 and stored in distilled water at 4 °C prior to use (Wu et al. 2014c). To prepare plasticized BC, BC membranes were first dehydrated in a centrifuge at 3000 r/min for 5 min. Then the semi-dry BC membranes were immersed in glycerol aqueous solutions of 1, 1.5 and 2 wt% for 24 h. Next, the membranes were placed on a plastic plate for natural drying by air. The products were named BC/1%G, BC/1.5%G and BC/2%G, respectively. The BC/PEG membranes were prepared by the same method, and named BC/1%PEG, BC/1.5%PEG and BC/2%PEG, respectively.

Characterization of the plasticized dry BC membranes

The morphology of BC/G and BC/PEG was examined by a field emission scanning electron microscope (FE-SEM) (Zeiss, Germany) operating at 5 kV. Prior to SEM observation, the membranes were freeze-dried for 24 h and coated with a thin layer of gold.

The chemical interactions between BC and the plasticizers were studied using a Fourier transform infrared spectroscope (FT-IR) (Thermo Scientific Nicolet 6700). The membranes were dried in air. The spectra were recorded in the range of 4000–600 cm^{-1}.

Thermo-gravimetry (TG) experiments were performed on a Shimadzu TGA 50 analyzer. The temperature was heated from room temperature to 600 °C under a nitrogen atmosphere. The heating rate was 10 °C/min. For each test, 10 mg of the samples was used, and the result was the average of three tests.

The surface roughness (Ra) of the BC/G and BC/PEG was tested using a laser confocal scanning microscope (Olympus LEXT OLS4000, Japan). For each sample, 5 points were randomly picked and tested. The water contact angles (WCAs) of the membranes were tested on a Contact Angle System OCA (Kruss, Germany). The volume of each liquid drop was 2 μL. The surfaces of membranes were kept smooth and dry in the Ra and WCA tests.

The tensile stress-strain properties of the membranes were measured with a TA-HD plus Texture Analyzer (Stable Micro Systems Co. Ltd, UK) at room temperature. Three samples from one membrane were cut into dumbbell shapes with a width of 4 mm and length of 50 mm following ISO standards[ISO37:2005(E)] (Qiao et al. 2015). The loading rate was kept at a strain rate of 100 mm/min. Three samples were measured to obtain the average and standard deviation (Akturk et al. 2011).

Water absorption and water retention

Dry BC, BC/G and BC/PEG were vacuum-dried for 24 h before testing their water absorption capacity (WA) and water retention rate (WR). The WA of the membranes was tested by a gravimetric method (Akturk et al. 2011). Initially, the membranes were cut into 4 cm × 4 cm pieces and the dry weights (W_d) were measured. Then each sample was immersed in 200 ml of deionized water at room temperature (25 °C). The weight of each sample was measured after removing excess surface water (W_s). The WA was calculated using the following equation:

$$WA(\%) = (W_s - W_d)/W_d \times 100\% \qquad (1)$$

The water retention capacity of the membranes was evaluated by water retention tests (Bodhibukkana et al. 2006). The initial weights of dry BC, BC/G and BC/PEG were measured (W_d). Then the samples were immersed in deionized water for 24 h. After that, the surface water on the samples was wiped away with filter paper and the samples were placed in centrifuge tubes and centrifuged at 500 r/min for 3 min. Then the samples were taken out and weighed again (W_w). The WR was defined by the following equation (Lin et al. 2013):

$$WR(\%) = (W_w - W_d)/W_d \times 100\% \qquad (2)$$

Triplicate samples from one membrane were tested.

Water vapor transmission

The WVTs of the BC/G and BC/PEG were determined according to the ASTM E96 standard method (Bodhibukkana et al. 2006). The WVTs of the membranes were determined according to YY/T 0471.2. The tests were carried out on a PERME W3/010 water vapor transmission instrument (Jinan Lan Guang Electrical

and Mechanical Technology Co., Ltd) (Fig. 1A). The test temperature and humidity were 38 °C and 90%RH, respectively. The test warm-up time was 2 h and the weighing interval was 120 min. To take into consideration the water absorbed by the membranes, the mass changes of the membranes after the tests were divided by the sample area and test time and converted into WVTs, and then deducted from the results. Triplicate tests were carried out.

Resistance to bacteria

The process of the bacteria resistance experiment is illustrated in Fig. 1B. First, *Staphylococcus aureus (S. aureus)* was inoculated on a sterile agar plate in a petri dish in an "x" shape. Each line of the "x" was less than 2 cm. Afterwards, the membrane (at least 5 cm × 5 cm in surface area) was placed on the petri dish covering the "x" shape. Then another petri dish with sterile agar plate was placed on top of the membrane. A 100 g weight was then added on the upper petri dish to form a continuous pressure. This set was incubated at 37 °C for 24 h. Finally, the upper petri dish was taken down, capped and incubated at 37 °C for another
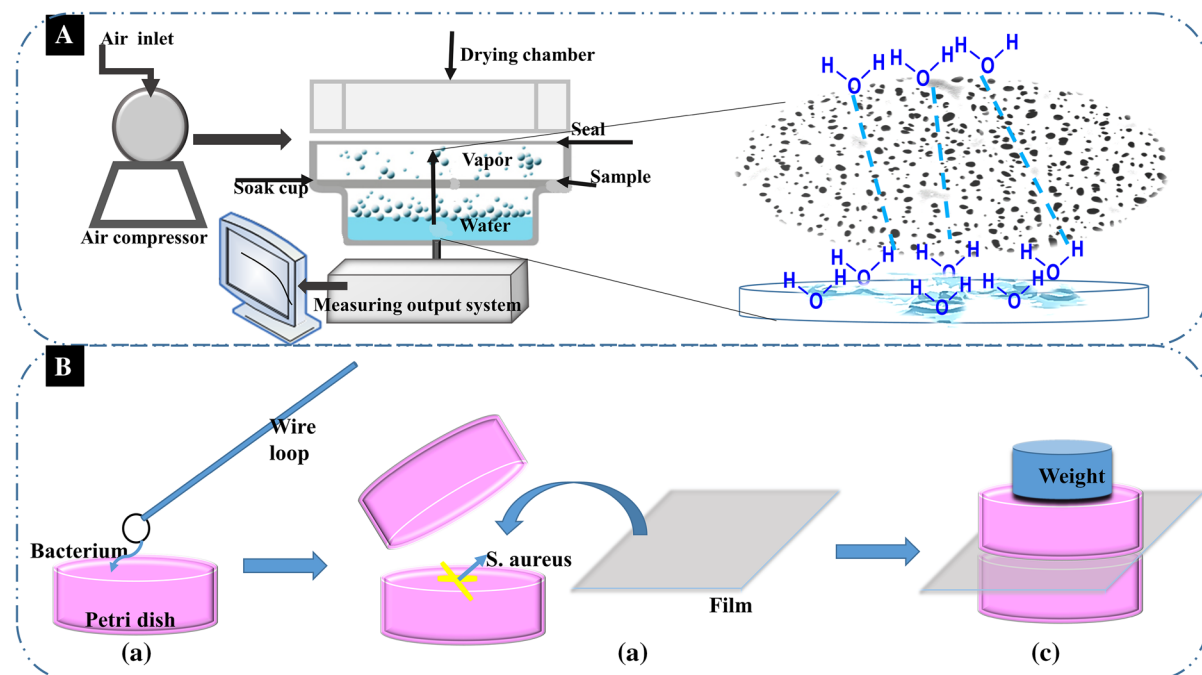

Fig. 1 **A** Schematic of the WVTR test. **B** The procedure of the resistance against bacteria test: (a) first step; (b) second step; (c) final step

24 h before being examined for the *S.aureus* colony. Triplicate tests were carried out.

Results and discussion

Mechanism of plasticization

The mechanism of plasticization is illustrated in Fig. 2. BC has a network structure composed of nano fibers. Upon drying, the three-dimensional structure collapses to a densely packed structure, and large amounts of hydrogen bonds form between the fibers (Bäckdahl et al. 2006). The large amounts of hydrogen bonds limit the relative movement between the fibers, making dry BC a very strong and brittle material. After incorporating plasticizers, namely glycerol and PEG, the plasticizers not only cover the surface but also penetrate the BC fiber networks. The plasticizers form hydrogen bonds with the BC fibers, preventing the fibers from forming too many hydrogen bonds with each other. As a result, the space between the fibers is enlarged, the interaction between the fibers is decreased, and the relative movements between the

Fig. 2 Illustrations of the microstructures of BC, BC/ G and BC/PEG
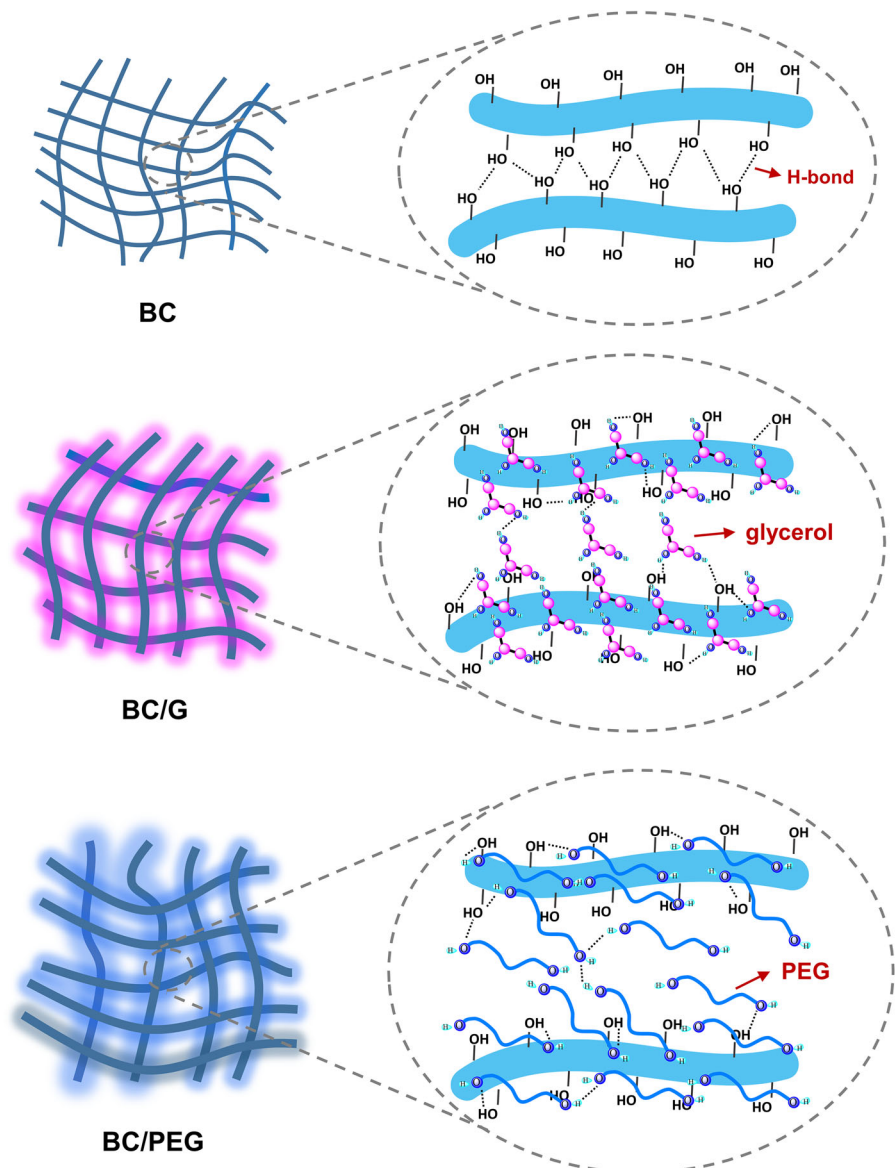
fibers are easier (Bocqué et al. 2016; Ghasemlou et al. 2011; Sanyang et al. 2015).

The FT-IR spectra of BC, BC/G and BC/PEG are shown in Fig. 3. For the spectrum of BC, the characteristic absorption at 3345 cm^{-1} is attributed to the O-H stretching vibrations of the hydroxyl groups present in BC; the absorption around 2895 cm^{-1} is because of the C-H stretching vibrations; the peak at 1645 cm^{-1} results from the symmetrical stretching of –OH (Maréchal and Chanzy 2000; Vasconcelos et al. 2017). For the spectra of BC/G (Fig. 3a), the absorption at 3726–2997 and 1645 cm^{-1} was greatly enchanced, which is in accordance with the spectrum of glycerol. The absorption intensified with the increase in glycerol content. This is due to the large amounts of hydroxyl groups in glycerol. The double peaks at 2929 and 2884 cm^{-1} are ascribed to the C–H stretching

vibrations in glycerol molecules. The absorption around 1109 and 1032 cm^{-1} are ascribed mainly to the C–C and C–O stretching vibrations in glycerol molecules, respectively (Chen et al. 2008). These facts together suggest that BC is compounded with glycerol. For the spectra of BC/PEG (Fig. 3b), the absorption at 3700–3008 and 1645 cm^{-1} also intensified with the increase in PEG content, which is due to the hydroxyl groups in PEG. However, compared with BC/G, the absorption was much weaker. This is because the content of hydroxyl groups in PEG is much lower than that in glycerol.

Morphological characterization

SEM was used to study the microstructure of the membranes. Dry BC showed a fibrous structure (Fig. 4a, b). The nanofibers were densely stacked,

Fig. 3 FT-IR spectra of BC/G (**a**) and BC/PEG (**b**). For interpretation of the references to color in this figure legend, the reader is referred to the web version of this article
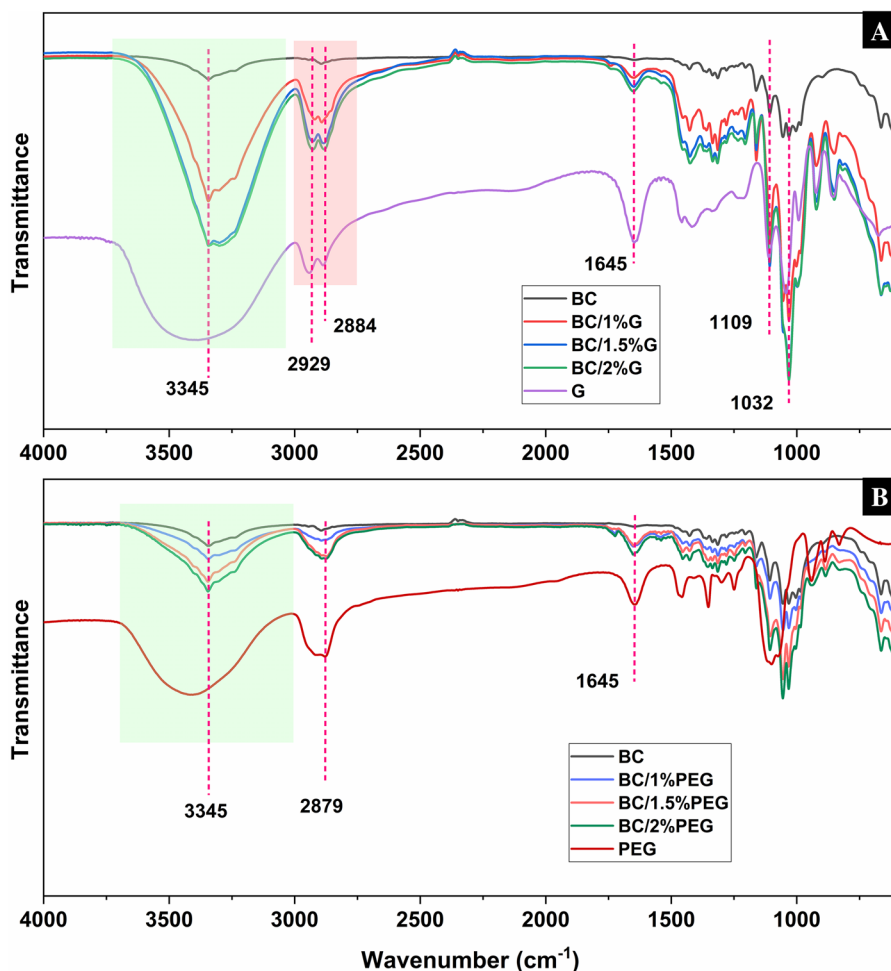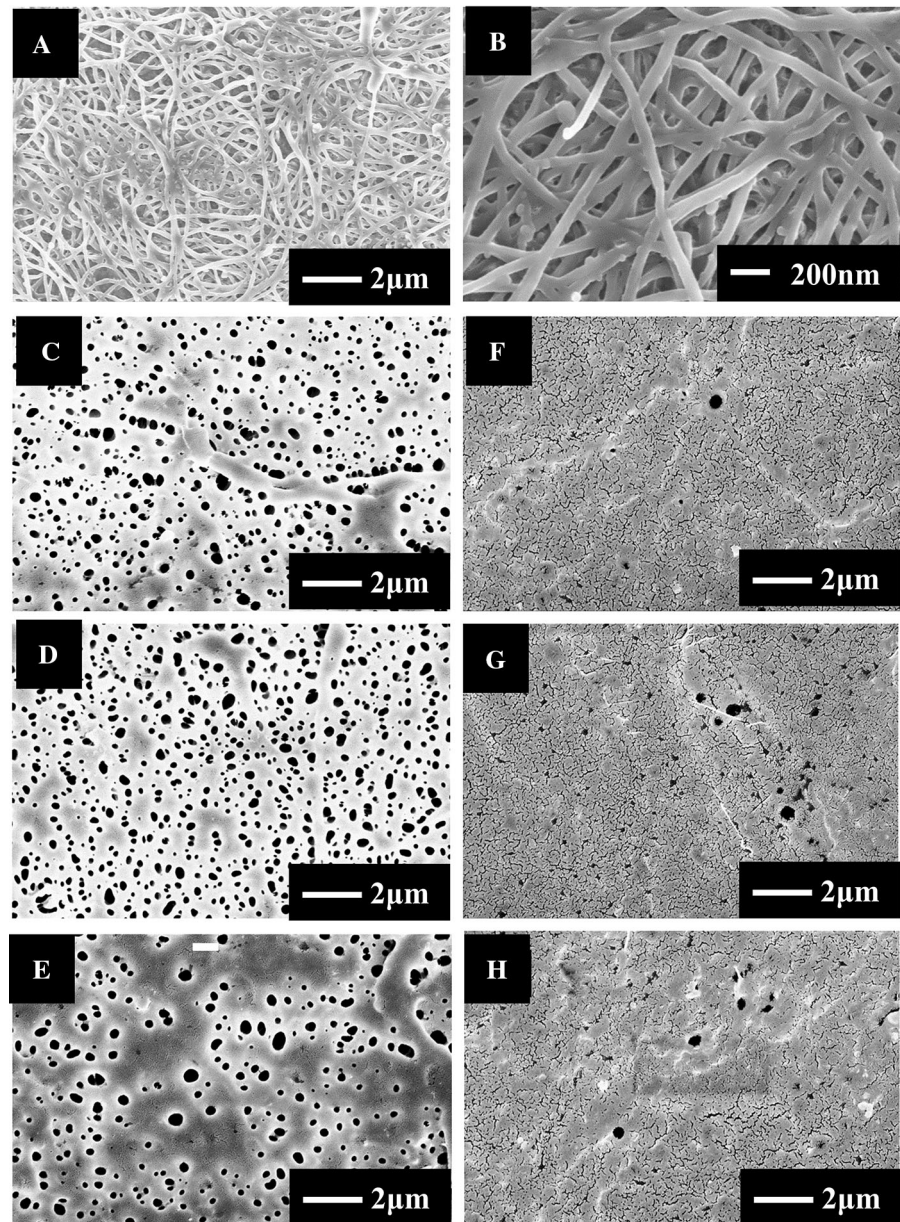
Fig. 4 SEM images of BC(**a**, **b**), BC/1%G (**c**), BC/1.5%G (**d**), BC/2%G (**e**), BC/1%PEG (**f**), BC/1.5%PEG (**g**) and BC/2%PEG (**h**)

making the relative movements between the fibers very difficult (Bäckdahl et al. 2006; Lamboni et al. 2016). In contrast, no obvious fibrous structure were observed for BC/G or BC/PEG, This can be ascribed to the coverage of plasticizers on the BC fibers (Cai and Kim 2010). As can be seen, BC/G and BC/PEG were homogeneous with no visible signs of aggregation. This means that there is a good compatibility between the plasticizer and BC. Additionally, BC/G showed an abundant number of pores (Fig. 4c–e), while fewer

pores and more micro cracks were observed for BC/PEG (Fig. 4f–h). These structures can contribute to the exchange of gas and the absorption of wound exudate (Yin et al. 2012).

The three-dimensional surface images of BC, BC/G and BC/PEG are shown in Fig. 5a–g. The corresponding surface roughness are shown in Fig. 5h. As can be seen, dry BC showed a relatively smooth surface, with a low surface roughness of only 0.125 μm. This can be explained by the densely stacked structure as shown in
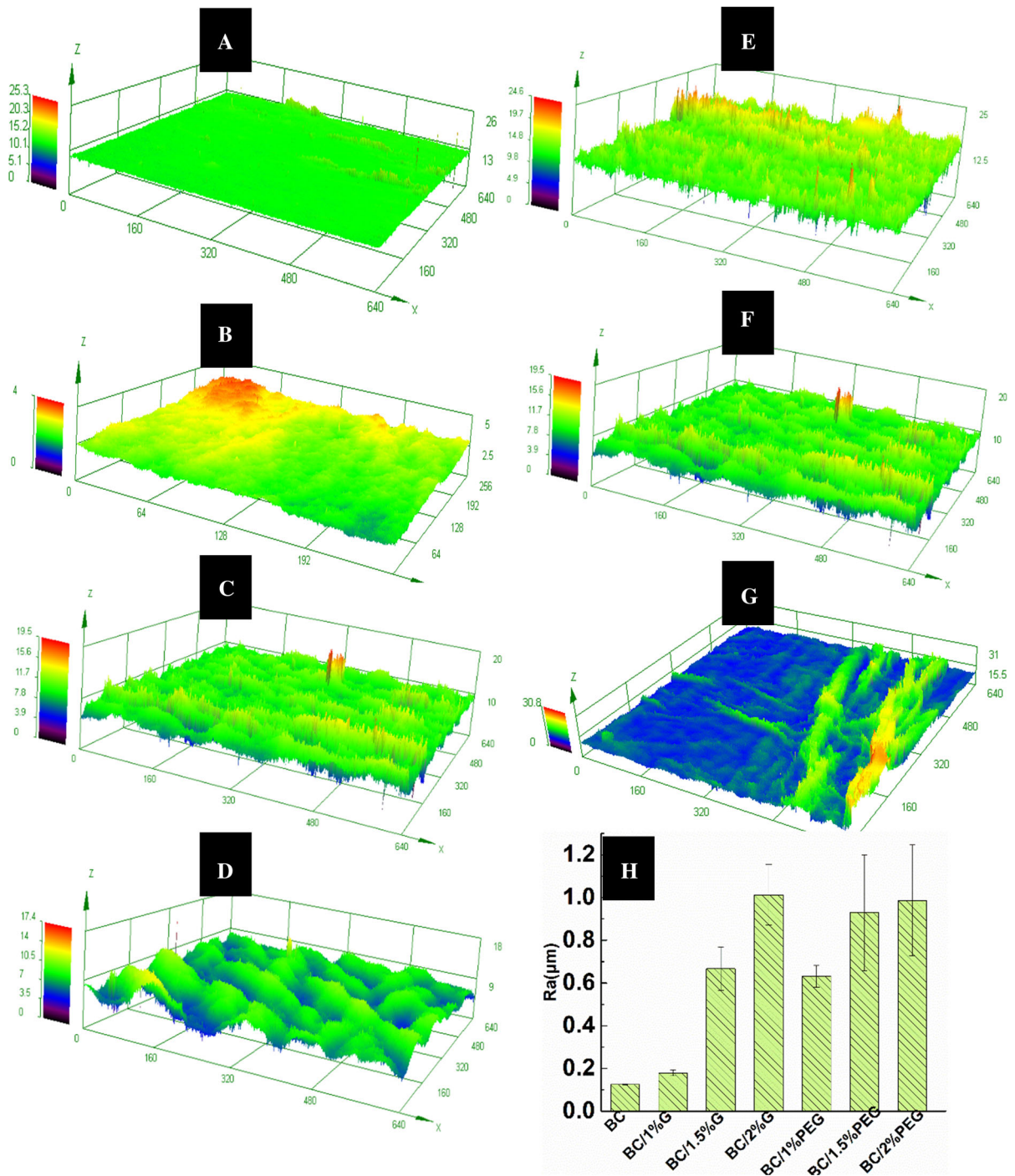
Fig. 5 Three-dimensional surface images of BC (**a**), BC/1%G (**b**), BC/1.5%G (**c**), BC/2%G (**d**), BC/1%PEG (**e**), BC/1.5%PEG (**f**) and BC/2%PEG(g); (**h**) membranes roughness

Fig. 4a. After the incorporation of plasticizers, the roughness of the membranes significantly increased. The surface roughness of BC/G and BC/PEG both increased with the rise in plasticizer content. At 2% plasticizer content, the surface roughness of BC/G and BC/PEG were 1.01 μm and 0.987 μm, respectively

(Fig. 5h). The increased surface roughness may result from the larger space between the BC fibers of BC/G and BC/PEG. The larger surface roughness is beneficial for cell growth and may therefore benefit the wound healing (Faucheux et al. 2004).

The contact angle with water (CA) of a wound dressing reflects its ability to absorb wound fluid. The CAs of dry BC, BC/G and BC/PEG are shown in Fig. 6a. Dry BC showed good hydrophilicity with a small CA of 34.1°, which was derived from the large amounts of hydroxyl groups present in dry BC (Fig. 6b). Adding 1% of glycerol increased the CA to 60°. This is due to the fact that glycerol has a comparatively smaller hydroxyl content than BC. However, further adding glycerol led to a decrease of CA. This is because that, as the amount of plasticizers increased, the amount of hydroxyls on the surface of the membrane also increased (Fig. 6c). As a result, the hydrophilia in the CA decreased. For BC/2%G, the CA was about 43.4°, which is very close to that of dry BC. The CAs of BC/PEG also showed a similar pattern. However, because PEG has an even smaller hydroxyl content than glycerol, at the same content, BC/PEG has a larger CA than BC/G. These results show that the hydrophilicity of BC/G and BC/PEG can be tailored for different demands.

Mechanical property and thermal stability

Tensile stress-strain experiments were used to study the mechanical behavior of the plasticized membranes. As can be seen in Fig. 7, dry BC had a high tensile strength of 165 MPa. However, the elongation at break (E %) of dry BC was only 3.4%. This indicates that it is highly brittle. Comparatively, BC/G showed lower tensile strength, but the E% value was much higher (Fig. 7a). With the glycerol content increasing from 1 to 2%, the tensile strength decreased from 103 to 56.8 MPa, which is still relatively high. Meanwhile, the E% values increased from 16.7 to 28.1%, indicating that the flexibility of BC/G was effectively improved. This can be explained by the inner space increase caused by the adding of plasticizer (Sothornvit and Krochta 2001; Sreedhar et al. 2005). As is shown in Fig. 2, the fibers of dry BC are closely stacked and formed quantities of H-bonds with each other. There is little space between the fibers and the fibers are locked to each other. Therefore, the tensile strength is very high and the E% value is small. With the addition of plasticizer, the plasticizer molecules enter the space between the fibers and form H-bonds with them (Azadimanesh and Mohammadi 2015). The H-bonds between the fibers are effectively decreased and the space between the BC fibers is increased. As a result, the fibers can move away from each other and the E% value increases.

BC/PEG showed the similar variation (Fig. 7b). However, compared with BC/G, BC/PEG presented smaller tensile strength and larger E% values. This might be because that the PEG molecules has a much smaller hydroxyl density than Glycerol. Consequently the there are less H-bonds between the fibers in BC/PEG than in BC/G. Therefore, the interaction between the fibers are weaker and the relative movement is
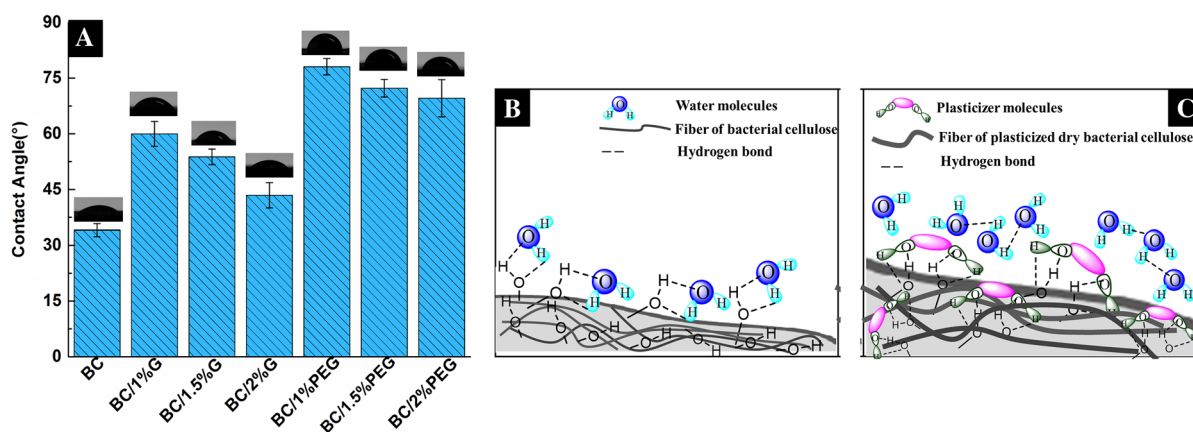

Fig. 6 (**a**) Contact angles of the membranes; schematic illustration of the surface hydrophilicity of dry BC (**b**) and plasticized dry BC (**c**)
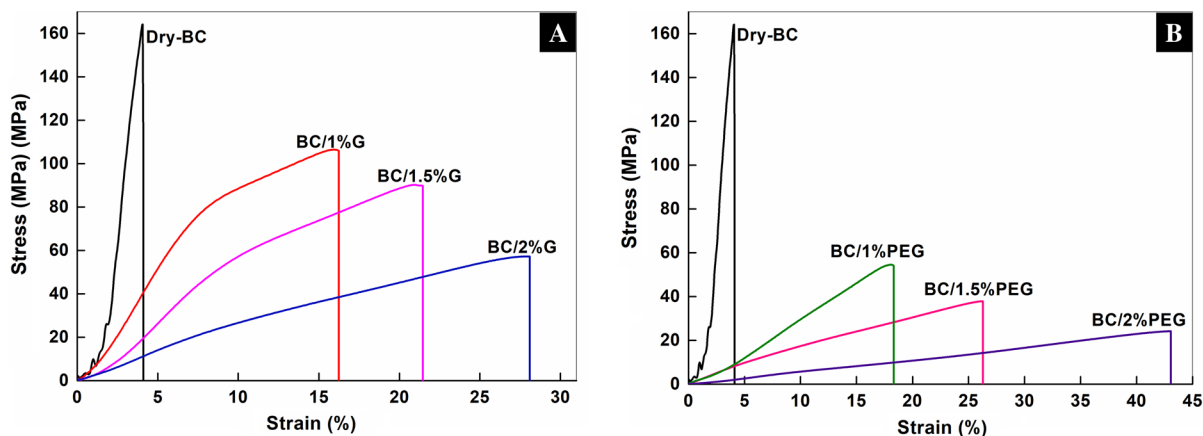
Fig. 7 Tensile stress-strain curves of BC/G (**a**) and BC/PEG (**b**)

easier. The tensile results show that B/G and BC/PEG had good mechanical properties and that BC membranes of different mechanical properties can be achieved by verifying the plasticizer type and content. This is beneficial for their application as wound dressings as they can withstand the stress during handling and provide mechanical protection to the wound (Archana et al. 2013). The detailed results of the mechanical tests are presented in Table 1.

The thermal stability of the membranes were assessed by TG analysis, as shown in Fig. 8. For all membranes, the weight losses in the range of 30–100 °C are attributed to the loss of absorbed water. BC presented the one-stage decomposition at 250 °C, which is attributed to the degradation of the main cellulose skeleton (Li et al. 2010). In comparison, both BC/G and BC/PEG display two weight loss stages. For BC/G, the first stage occurs at 120–270 °C. This is due to the degradation of the glycerol-gather phase in BC/G (Montero et al. 2017). For BC/PEG, the first weight loss stage occurs at 130–290 °C, which corresponds to the decomposition of PEG (Mishra et al. 2017). Both BC/G and BC/PEG have the second

weight loss stage at 290–400 °C. This is well consistent with that of BC. The TG results show that both BC/G and BC/PEG are stable before 100 °C. This means they have good stability in their application as wound dressings.

Water absorption and water retention performance

Water absorption capacity (WA) is one of the vital criteria for wound dressing applications. The WA results of dry BC, BC/G and BC/PEG are shown in Fig. 9a, b. As can be seen, dry BC had a very low WA. This is because the fibers of dry BC are tightly locked to each other by H-bonds and there is much smaller space inside the membrane (de Souza et al. 2013). In addition, the H-bonds between the fibers are so strong that water molecules are not able to break them. As a result, the ability of dry BC to absorb water was limited by its low inner space. In contrast, both BC/G and BC/PEG showed high water absorption, which were more than 40 times higher than that of dry BC. This can still be explained by their inner structure. After incorporation of plasticizers, the glycerol and

Sample	Tensile strength (Mpa)	Modules (Mpa)	Elongation at breake (%)
Dry-BC	165 ± 4.2	4032 ± 91.2	3.46 ± 0.09
BC/1%G	103 ± 2.6	698.3 ± 16.2	16.7 ± 0.65
BC/1.5%G	98.7 ± 2.5	448.2 ± 10.7	21.5 ± 0.97
BC/2%G	56.8 ± 1.4	217.4 ± 6.35	28.1 ± 0.63
BC/1%PEG	55.0 ± 1.6	307.6 ± 6.26	18.4 ± 0.41
BC/1.5%PEG	37.8 ± 0.41	151.1 ± 3.39	37.7 ± 1.28
BC/2%PEG	24.1 ± 0.61	56.80 ± 1.05	43.2 ± 1.12

Table 1 Mechanical properties of dry BC, BC/G and BC/PEG
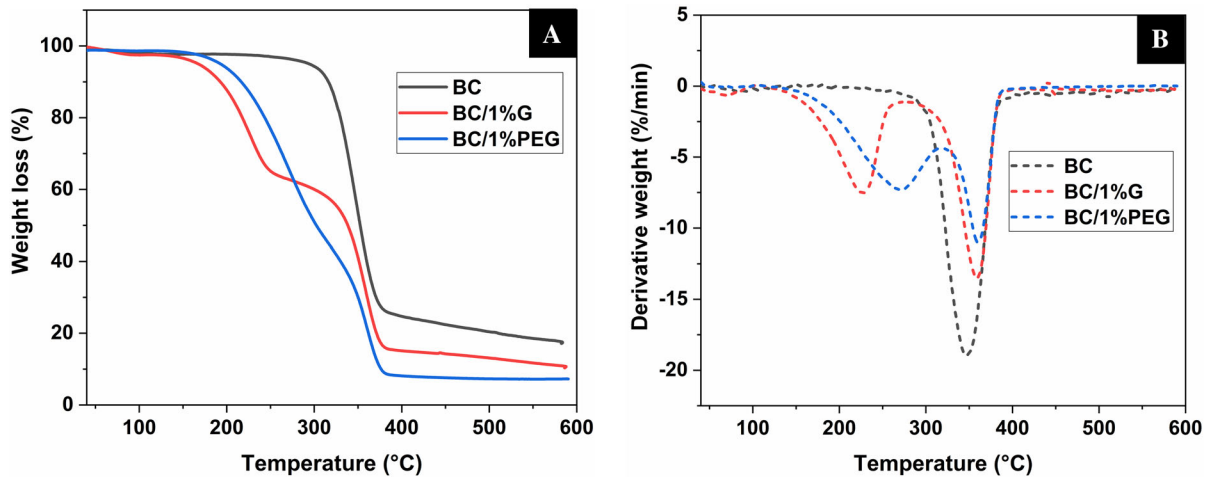
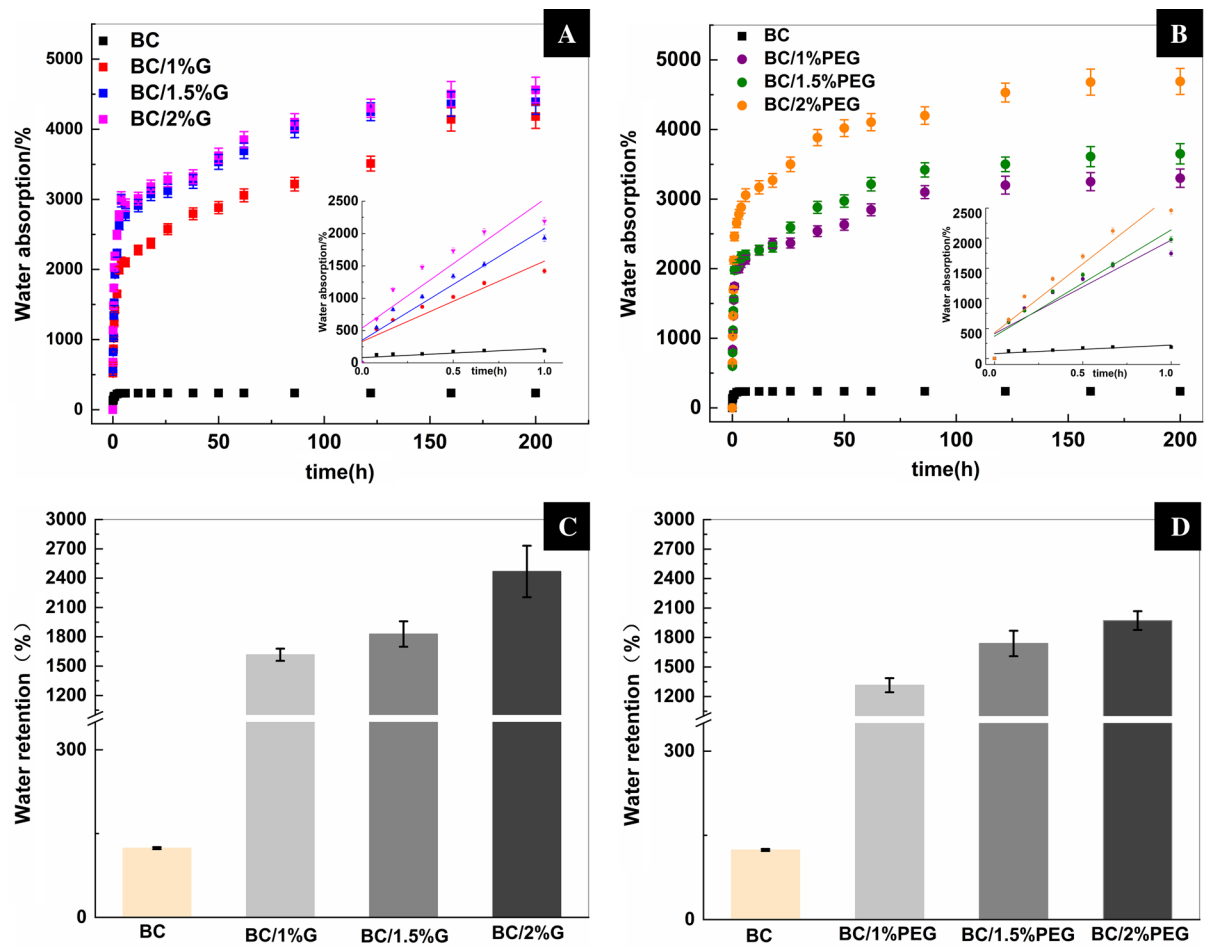**Fig. 8** TG (**a**) and DTG (**b**) curves of BC, BC/G and BC/PEG

Fig. 9 Time-dependent water absorption of BC/G (**a**) and BC/PEG (**b**); time-dependent water retention of BC/G (**c**) and BC/PEG (**d**)

PEG molecules reduces the H-bonds between the fibers and effectively enlarge the volume space between them. As a result, the membranes have more space to hold water (Stumpf et al. 2013). In addition, upon absorbing water, the inner space is further enlarged because the impediment of the H-bonds is much smaller. Therefore, the water absorption of the plasticized dry BC membranes was greatly improved. However, there are differences between BC/G and BC/PEG. For BC/G, water absorption did not change much when the glycerol content was further increased from 1.5 to 2%. Comparatively, the water absorption of BC/PEG was obviously improved with the same content change. This might originate from the size effect of the plasticizers.

The water retention rate (WR) is another important parameter for wound dressings. As shown in Fig. 9c, d, BC shows a poor WR of 237%, which is derived from its low water absorption. In comparison, BC/2%G has a high WR of 4560%, which is 18.2 times higher than that of BC. With the increase of glycerol content from 1 to 2%, the WR increased from 1616 to 2468%. This might be due to the higher water absorption at higher glycerol content (Hsieh 1995; Montero et al. 2017). BC/PEG also showed similar pattern, but its WR was smaller than BC/G at the same plasticizer content. This may be due to the lower hydroxyl content of PEG, which leads to a weaker interaction with water molecules.

Water vapor transmission and resistance to bacteria

A WVT of 2500 $g/m^2 \cdot 24$ h would provide an adequate level of moisture without risking wound dehydration or accumulating excessive exudates (Mi et al. 2001).

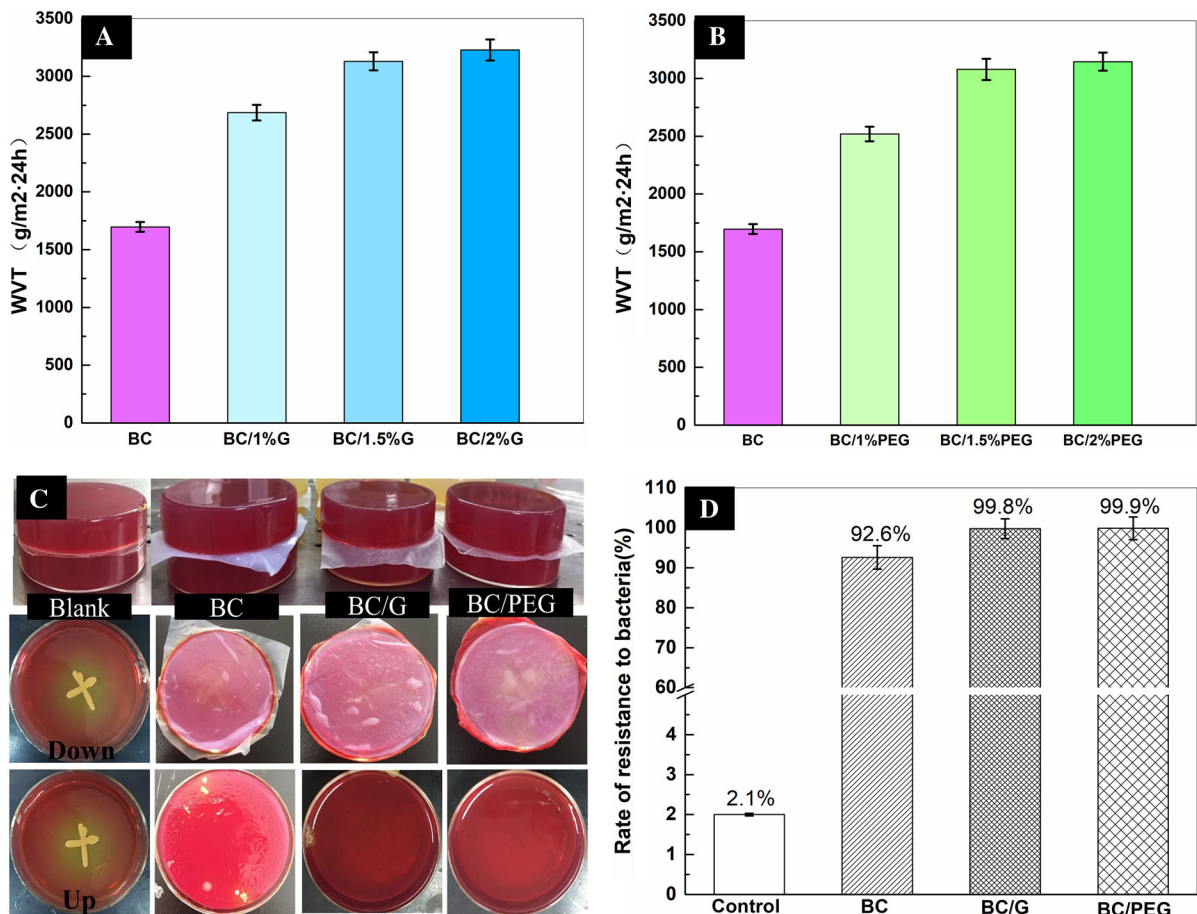**Fig. 10** **a**, **b** WVTs of BC/G and BC/PEG; **c** the photograph of resistance to bacteria; **d** values of resistance to bacteria rate

As can be seen in Fig. 10a, dry BC has a low WVT of 1696 g/m^2·24 h. Comparatively, BC/1%G and BC/1%PEG membranes both had WVTs close to 2500 g/m^2·24 h. The water vapor transmission through a film is dependent on the diffusion rate and solubility of water molecules in the film structure (Nawab et al. 2016). Therefore, the higher WVTs of the BC/G and BC/PEG can be explained by two reasons. On one hand, because BC/G and BC/PEG have more hydroxyl groups which can interact with water by hydrogen bonds, more water molecules can enter the membranes. On the other hand, BC/G and BC/PEG have larger inner space and a porous structure, which facilitate the transmission of water molecules (Lainioti et al. 2016). Therefore, the WVTs of BC/G and BC/PEG are much higher than that of dry BC. With the increase of plasticizer content, the WVT also increased. Hence, the WVT of the membranes can be tuned by varying the plasticizer content for different wound types.

The rate of resistance to bacteria (RB) of a wound dressing is a vital character. Figure 10c shows the bacteria resistance effect of different membranes, and the RB results are presented in Fig. 10d. As can be seen, all membranes showed a good resistance to bacteria. The RBs of BC, BC/G and BC/PEG are 92.6%, 99.8% and 99.9%, respectively. This is because the pore diameters of these membranes are much smaller than that of bacteria and bacteria have no way to pass through the membranes (Mi et al. 2001). However, since dry BC is brittle, there can be cracks on the dry BC membranes. As a result, some bacteria could pass the dry BC membrane through the cracks. Comparatively, the toughness of BC/G and BC/PEG is effectively improved by the plasticizers, and no cracks can easily form on these membranes. Therefore, both BC/G and BC/PEG have a good RB of near 100%. This further demonstrates their promising potential as wound dressings.

Conclusion

In this study, BC/G and BC/PEG were prepared using two biocompatible plasticizers with different molecular weight and hydroxyl content. Glycerol and PEG not only covered the BC microfibers but also enlarged the free space between the fibers, forming a porous structure. The toughness of BC/G and BC/PEG were effectively improved. The water absorption and water retention capacities of BC/G and BC/PEG were significantly higher than dry BC. The highly porous structure of the plasticized dry BC membranes enhanced the water vapor transmission rates of the membranes. The plasticized dry BC membranes showed excellent resistance against bacteria. The different performances of the two plasticized dry BC membranes originate from the different nature of the plasticizers, and can be tuned to adapt to different applications.

Compliance with ethical standards

Conflict of Interest The authors declare that they have no conflict of interest.

References

Akturk O, Tezcaner A, Bilgili H, Deveci MS, Gecit MR, Keskin D (2011) Evaluation of sericin/collagen membranes as prospective wound dressing biomaterial. J Biosci Bioeng 112:279–288

Almeida IF et al (2013) Bacterial cellulose membranes as drug delivery systems: an in vivo skin compatibility study. European Journal of Pharmaceutics & Biopharmaceutics Official Journal of Arbeitsgemeinschaft Fur Pharmazeutische Verfahrenstechnik E V 86:332–336

Andrade FK, Costa R, Domingues L, Soares R, Gama M (2010) Improving bacterial cellulose for blood vessel replacement: functionalization with a chimeric protein containing a cellulose-binding module and an adhesion peptide. Acta Biomater 6:4034–4041

Archana D, Singh BK, Dutta J, Dutta P (2013) In vivo evaluation of chitosan–PVP–titanium dioxide nanocomposite as wound dressing material. Carbohydr Polym 95:530–539

Azadimanesh F, Mohammadi N (2015) A plasticizer index to universally correlate the normalized work of fracture and elastic modulus of plasticized cellulose triacetates. Carbohydr Polym 130:316–324

Bäckdahl H, Helenius G, Bodin A, Nannmark U, Johansson BR, Risberg B, Gatenholm P (2006) Mechanical properties of bacterial cellulose and interactions with smooth muscle cells. Biomaterials 27:2141–2149

Bocqué M, Voirin C, Lapinte V, Caillol S, Robin J-J (2016) Petro-based and bio-based plasticizers: chemical structures to plasticizing properties. J Polym Sci Part A Polym Chem 54(1):11–33

Bodhibukkana C, Srichana T, Kaewnopparat S, Tangthong N, Bouking P, Martin GP, Suedee R (2006) Composite membrane of bacterially-derived cellulose and molecularly

imprinted polymer for use as a transdermal enantioselective controlled-release system of racemic propranolol. J Controlled Release 113:43–56

Bu Y et al (2018) Ultra-thin bacterial cellulose/poly (ethylenedioxythiophene) nanofibers paper electrodes for all-solid-state flexible supercapacitors. Electrochim Acta 271:624–631

Cai Z, Kim J (2010) Bacterial cellulose/poly (ethylene glycol) composite: characterization and first evaluation of biocompatibility. Cellulose 17:83–91

Chen P, Tian H, Zhang L, Chang PR (2008) Structure and properties of soy protein plastics with ε-caprolactone/glycerol as binary plasticizers. Ind Eng Chem Res 47(23):9389–9395

Cobos M, González B, Fernández MJ, Fernández MD (2017) Chitosan–graphene oxide nanocomposites: Effect of graphene oxide nanosheets and glycerol plasticizer on thermal and mechanical properties. J Appl Polym Sci 134(30):45092

Cui Q, Zheng Y, Lin Q, Song W, Qiao K, Liu S (2014) Selective oxidation of bacterial cellulose by NO_2-HNO_3. RSC Adv 4:1630–1639. https://doi.org/10.1039/c3ra44516j

de Souza CF, Lucyszyn N, Woehl MA, Riegel-Vidotti IC, Borsali R, Sierakowski MR (2013) Property evaluations of dry-cast reconstituted bacterial cellulose/tamarind xyloglucan biocomposites. Carbohydr Polym 93:144–153

Díaz-Calderón P, MacNaughtan B, Hill S, Foster T, Enrione J, Mitchell J (2018) Changes in gelatinisation and pasting properties of various starches (wheat, maize and waxy maize) by the addition of bacterial cellulose fibrils. Food Hydrocoll 80:274–280

Faucheux N, Schweiss R, Lützow K, Werner C, Groth T (2004) Self-assembled monolayers with different terminating groups as model substrates for cell adhesion studies. Biomaterials 25:2721–2730

Ghasemlou M, Khodaiyan F, Oromiehie A (2011) Physical, mechanical, barrier, and thermal properties of polyol-plasticized biodegradable edible film made from kefiran. Carbohydr Polym 84(1):477–483

Hsieh Y-L (1995) Liquid transport in fabric structures. Text Res J 65:299–307

Jayakumar R, Prabaharan M, Kumar PS, Nair S, Tamura H (2011) Biomaterials based on chitin and chitosan in wound dressing applications. Biotechnol Adv 29:322–337

Khamrai M, Banerjee SL, Kundu PP (2017) Modified bacterial cellulose based self-healable polyeloctrolyte film for wound dressing application. Carbohydr Polym 174:580–590

Lainioti GC, Bounos G, Voyiatzis GA, Kallitsis JK (2016) Enhanced water vapor transmission through porous membranes based on melt blending of polystyrene sulfonate with polyethylene copolymers and their cnt nanocomposites. Polymers 8:190

Lamboni L, Li Y, Liu J, Yang G (2016) Silk sericin-functionalized bacterial cellulose as a potential wound-healing biomaterial. Biomacromol 17:3076–3084

Li S-M, Jia N, Zhu J-F, Ma M-G, Sun R-C (2010) Synthesis of cellulose–calcium silicate nanocomposites in ethanol/water mixed solvents and their characterization. Carbohydr Polym 80:270–275

Li Z, Qiu J, Shi Y, Pei C (2018) Wettability-switchable bacterial cellulose/polyhemiaminal nanofiber aerogels for continuous and effective oil/water separation. Cellulose 25:2987–2996

Liakos I et al (2015) Fibrous wound dressings encapsulating essential oils as natural antimicrobial agents. J Mater Chem B 3:1583–1589

Lin W-C, Lien C-C, Yeh H-J, Yu C-M, S-h Hsu (2013) Bacterial cellulose and bacterial cellulose–chitosan membranes for wound dressing applications. Carbohydr Polym 94:603–611

Lin Q, Zheng Y, Wang G, Shi X, Zhang T, Yu J, Sun J (2015) Protein adsorption behaviors of carboxymethylated bacterial cellulose membranes. Int J Biol Macromol 73:264–269. https://doi.org/10.1016/j.ijbiomac.2014.11.011

Luo H, Xiong G, Wan Y (2014) In situ phosphorus K-edge X-ray absorption spectroscopy studies of calcium–phosphate formation and transformation on the surface of bacterial cellulose nanofibers. Cellulose 21:3303–3309

Maréchal Y, Chanzy H (2000) The hydrogen bond network in I β cellulose as observed by infrared spectrometry. J Mol Struct 523:183–196

Mi F-L, Shyu S-S, Wu Y-B, Lee S-T, Shyong J-Y, Huang R-N (2001) Fabrication and characterization of a sponge-like asymmetric chitosan membrane as a wound dressing. Biomaterials 22:165–173

Mishra SK, Mary DS, Kannan S (2017) Copper incorporated microporous chitosan-polyethylene glycol hydrogels loaded with naproxen for effective drug release and anti-infection wound dressing. Int J Biol Macromol 95:928–937

Montero B, Rico M, Rodríguez-Llamazares S, Barral L, Bouza R (2017) Effect of nanocellulose as a filler on biodegradable thermoplastic starch films from tuber, cereal and legume. Carbohydr Polym 157:1094–1104

Napavichayanun S, Yamdech R, Aramwit P (2018) Development of bacterial cellulose incorporating silk sericin, polyhexamethylene biguanide, and glycerin with enhanced physical properties and antibacterial activities for wound dressing application. Int J Polym Mater Polym Biomater 67:61–67

Nawab A, Alam F, Haq MA, Hasnain A (2016) Biodegradable film from mango kernel starch: Effect of plasticizers on physical, barrier, and mechanical properties. Starch-Stärke 68:919–928

Numata Y, Muromoto K, Furukawa H, Gong JP, Tajima K, Munekata M (2009) Nonvolatile and shape-memorized bacterial cellulose gels swollen by poly (ethylene glycol). Polym J 41:524

Qiao K et al (2015) Hydrophilic nanofiber of bacterial cellulose guided the changes in the micro-structure and mechanical properties of nf-BC/PVA composites hydrogels. Composites Sci Technol 118:47–54

Qiao H, Guo T, Zheng Y, Zhao L, Sun Y, Liu Y, Xie Y (2018) A novel microporous oxidized bacterial cellulose/arginine composite and its effect on behavior of fibroblast/endothelial cell. Carbohydr Polym 184:323–332

Qiu Y, Qiu L, Cui J, Wei Q (2016) Bacterial cellulose and bacterial cellulose-vaccarin membranes for wound healing. Mater Sci Eng C 59:303–309

Sanyang ML, Sapuan SM, Jawaid M, Ishak MR, Sahari J (2015) Effect of plasticizer type and concentration on tensile, thermal and barrier properties of biodegradable films based on sugar palm (Arenga pinnata) starch. Polymers 7:1106–1124

Sarhan WA, Azzazy HM, El-Sherbiny IM (2016) Honey/chitosan nanofiber wound dressing enriched with Allium sativum and Cleome droserifolia: enhanced antimicrobial and wound healing activity. ACS Appl Mater Interfaces 8:6379–6390

Shao W, Liu H, Wang S, Wu J, Huang M, Min H, Liu X (2016) Controlled release and antibacterial activity of tetracycline hydrochloride-loaded bacterial cellulose composite membranes. Carbohydr Polym 145:114–120

Silva NH et al (2014) Bacterial cellulose membranes as transdermal delivery systems for diclofenac: in vitro dissolution and permeation studies. Carbohydr Polym 106:264–269

Sothornvit R, Krochta JM (2001) Plasticizer effect on mechanical properties of β-lactoglobulin films. J Food Eng 50:149–155

Sreedhar B, Sairam M, Chattopadhyay D, Rathnam P, Rao D (2005) Thermal, mechanical, and surface characterization of starch–poly (vinyl alcohol) blends and borax-cross-linked films. J Appl Polym Sci 96:1313–1322

Stumpf TR, Pértile RA, Rambo CR, Porto LM (2013) Enriched glucose and dextrin mannitol-based media modulates fibroblast behavior on bacterial cellulose membranes. Mater Sci Eng C 33:4739–4745

Stumpf TR, Yang X, Zhang J, Cao X (2018) In situ and ex situ modifications of bacterial cellulose for applications in tissue engineering. Mater Sci Eng C 82:372–383

Sulaeva I, Henniges U, Rosenau T, Potthast A (2015) Bacterial cellulose as a material for wound treatment: properties and modifications. A review. Biotechnol Adv 33:1547–1571

Sun Y et al (2017) Mussel-inspired fabrication of a flexible free-standing membrane cathode for oxygen reduction in neutral media. J Electroanal Chem 799:377–385

Urbina L, Guaresti O, Requies J, Gabilondo N, Eceiza A, Corcuera MA, Retegi A (2018) Design of reusable novel membranes based on bacterial cellulose and chitosan for the filtration of copper in wastewaters. Carbohydr Polym 193:362–372

Vasconcelos NF, Feitosa JP, da Gama FM, Morais JP, Andrade FK, de Souza MD, de Freitas Rosa M (2017) Bacterial cellulose nanocrystals produced under different hydrolysis conditions: properties and morphological features. Carbohydr Polym 155:425–431

Wan Y, Yang Z, Xiong G, Luo H (2015) A general strategy of decorating 3D carbon nanofiber aerogels derived from bacterial cellulose with nano-Fe$_3$O$_4$ for high-performance flexible and binder-free lithium-ion battery anodes. J Mater Chem A 3:15386–15393

Wang Y et al (2018) Fabrication of nanofibrous microcarriers mimicking extracellular matrix for functional microtissue formation and cartilage regeneration. Biomaterials 171:118–132

Wu J et al (2014a) In situ synthesis of silver-nanoparticles/bacterial cellulose composites for slow-released antimicrobial wound dressing. Carbohydr Polym 102:762–771

Wu J et al (2014b) In situ synthesis of silver-nanoparticles/bacterial cellulose composites for slow-released antimicrobial wound dressing. Carbohydr Polym 102:762–771. https://doi.org/10.1016/j.carbpol.2013.10.093

Wu J, Zheng Y, Yang Z, Lin Q, Qiao K, Chen X, Peng Y (2014c) Influence of dialdehyde bacterial cellulose with the non-linear elasticity and topology structure of ECM on cell adhesion and proliferation. RSC Adv 4:3998–4009

Yang Z et al (2018) In-situ functionalization of poly (m-phenylenediamine) nanoparticles on bacterial cellulose for chromium removal. Chem Eng J 344:441–452

Ye Shan, Jiang Lei, Jimin Wu, Chen Su, Huang Chaobo, Liu Xiufeng, Shao Wei (2018) Flexible amoxicillin-grafted bacterial cellulose sponges for wound dressing. in vitro and in vivo evaluation. ACS Appl Mater Interfaces 10(6):5862–5870

Yin N et al (2012) Porous bacterial cellulose prepared by a facile surfactant-assisted foaming method in azodicarbonamide-NaOH aqueous solution. Mater Lett 81:131–134

Zhang X, He M, He P, Li C, Liu H, Zhang X, Ma Y (2018) Ultrafine nano-network structured bacterial cellulose as reductant and bridging ligands to fabricate ultrathin K-birnessite type MnO$_2$ nanosheets for supercapacitors. Appl Surf Sci 433:419–427